Accepted Manuscript

Dispersive seismic waves in a coal seam around the roadway in the presence of excavation damaged zone

Rafał Czarny, Michał Malinowski, Michał Chamarczuk, Mateusz Ćwiękała, Sławomir Olechowski, Zbigniew Isakow, Przemysław Sierodzki

https://doi.org/10.1016/j.ijrmms.2021.104937

Appeared in: International Journal of Rock Mechanics and Mining Sciences

Received date: 19 October 2020
Revised date: 12 September 2021
Accepted date: 6 October 2021
Available online: 12 October 2021
Version of Record: 12 October 2021

Please cite this article as:
Czarny, R., Malinowski, M., Chamarczuk, M., Ćwiękała, M., Olechowski, S., Isakow, Z., & Sierodzki, P. (2021). Dispersive seismic waves in a coal seam around the roadway in the presence of excavation damaged zone. *International Journal of Rock Mechanics and Mining Sciences*, *148*, 104937. https://doi.org/10.1016/j.ijrmms.2021.104937

Dispersive seismic waves in a coal seam around the roadway in the presence of excavation damaged zone

Rafał Czarny[1], Michał Malinowski[1,2], Michał Chamarczuk[1], Mateusz Ćwiękała[3], Sławomir Olechowski[3], Zbigniew Isakow[4], Przemysław Sierodzki[4]

[1]Institute of Geophysics, Polish Academy of Sciences, Ks. Janusza 64, 01-452 Warsaw, Poland.

E-mail: rczarny@igf.edu.pl (R. Czarny – corresponding author)

[2]Now at: Geological Survey of Finland (GTK), Vuorimiehentie 5, P.O. Box 96, 02151 Espoo, Finland

[3]PGG KWK ROW Ruch Rydułtowy coal mine, Leona 2, 44-280 Rydułtowy

[4]Centre of Technology Transfer EMAG, Leopolda 31, 40-189 Katowice

Highlights

- Dispersive waves behaviors within EDZ in a coal seam are derived by numerical simulations.
- In-mine experiment confirms roadway mode properties from modelling.
- Roadway mode dispersion curves correlate with the mechanical quality of the sidewall.
- Roadway mode can be useful in imaging and monitoring of the EDZ.

Keywords

Finite-difference methods, guided waves, coal seam, excavation damaged zone, dispersive waves, seismic channel waves, in-seam seismic, underground coal mining

Abstract

Excavation damaged zone (EDZ) is a fractured rock mass in the vicinity of the roadway. Knowing its elastic properties, such as seismic velocity, is crucial for the safety of underground mining. However, the seismic wavefield's complexity due to the low-velocity layer (e.g., a coal seam) makes it difficult to obtain reliable velocity estimates. Here, we study the influence of a roadway and EDZ on the seismic wavefield propagation inside the coal seam along the roadway close to the sidewall based on numerical simulation and in-seam seismic measurements. We focus on dispersive waves due to their dominant energetic contribution and, hence, application potential. We use the finite-difference method and viscoelastic model. First, we analyze seismic wave propagation within a simple rock-coal-rock model. Then, we add a cylindrically shaped roadway with 3-meter thick EDZ to the model. We observe a strong so-called roadway mode. Polarization analysis shows that such a mode in a horizontal plane in the center of the coal seam is the mix of Love-type channel and Rayleigh surface tunnel waves. Moreover, the EDZ causes a significant decrease of the group velocity, which turns out to be even lower than the lowest group velocity of the surface tunnel waves which travels solely in a coal seam. We also observe that the roadway mode with the presence of the EDZ is less dispersive, which can be useful with imaging the EDZ by those modes. Those roadway mode features were confirmed by the real seismic data from an underground experiment in the Rydułtowy coal mine in Poland. The rock mass deformation in the vicinity of the roadway strongly correlates with the roadway mode dispersion characteristic. Our study shows the great potential of using roadway mode in imaging and monitoring of underground excavations in the presence of a low-velocity layer.

1. Introduction

The presence of a thin, low-velocity layer in a high-velocity host rock favors the generation of frequency-dependent strong guided waves. Guided waves are found in different geological scenarios and at different scales. They can propagate inside the fault zone [1,2], plate contact of subduction zone [3], or in a coal seam [4]. The latter, so-called channel or seam waves, become useful in coal mining to detect and map disturbances in the front of longwall face. These waves build-up by the interference of body waves multiple reflections between a coal seam's floor and roof. As a consequence, two kinds of dispersive waves are produced: Love- and Rayleigh-type channel waves [5]. The first one is associated with SH body waves and the second with P-SV waves. The great benefit of the channel wave is that it is confined to the coal seam. Therefore, each change in the waveform is connected directly with a coal seam. Moreover, the characteristic feature of the seam wave is the strong Airy phase marked by the lowest group velocity [5]. Airy phase belongs to higher frequencies; therefore, it can probe the coal seam with high resolution. Even though the intrinsic attenuation in Airy phase is the highest the geometrical attenuation is the least [6]. Therefore, it can be recorded and identified from a long distance, particularly when the attenuation correction is applied [7]. Channel waves are also very sensitive to anisotropy [8-10], accounting for which can be necessary e.g. in the monitoring of small changes in the medium (aligned cracks, fractures). There are numerous studies on the channel waves propagation properties using 2-D [11-16] and 3-D [17-19] numerical modelling, as well as seismic field experiments [20-22]. However, there is still a lack of a dispersive wave behavior analysis in the roadway sidewall's vicinity.

There are two well-established in-seam seismic methods utilizing channel waves. The first one is based on the dispersive properties of channel waves when transmitted from one to another side of the longwall. The changes in Airy phase inform about changes in coal thickness or the presence of discontinuities. The thinner the coal seam, the higher the frequency of the Airy

phase and the smaller the dominating wavelength [23-25]. The second approach employs analysis of reflected channel waves from discontinuities in a coal longwall [26,27]. Usually, it is used to image the coal seam tectonic disturbances inside an existing longwall rather than ahead of a new roadway. Since look-ahead seismic for tunneling in hard rock has been successfully applied to body waves [28,29], recent developments have been proposed for coal mining, including channel waves as well [30-33].

The vast majority of applications have been focused on the Love-type channel wave, recorded by the horizontal component sensors in the center of a seam, where the fundamental mode is the strongest. It is because of the more practical two-component acquisition and more straightforward interpretation than for the Rayleigh-type channel wave [34]. However, Rayleigh-type channel wave can also be powerful when receivers are installed in ¼ of the seam thickness [14].

In-seam reflection seismic method requires installing geophones and sources in the same roadway. For such geometry, the common problem is the so-called roadway mode [35], the special type of dispersive wave generated by mixing channel waves with surface tunnel waves excited due to the free surface of a sidewall [36]. This wave overlaps with reflected channel wave mode and can hamper fault location [37]. It can be partially mitigated by applying a polarization filter [37] or mounting the geophones inside the boreholes a few meters away from the gallery face [27]. However, the latter is time-consuming and increases the cost of operations.

The roadway mode has been investigated numerically by Lagasse and Mason [35]. They found that it is similar to Love-type channel wave fundamental mode but with a 10% lower velocity. Roadway mode is also observed in Essen et al. [17] based on numerical simulation. By examining particle motion polarization between canter and upper border of the seam, they observed the dominant role of Rayleigh-type channel wave and Rayleigh tunnel surface wave

in the wavefield around the roadway. Similar observation to Lagasse and Mason [35] is confirmed by Krajewski et al. [37] based on real data.

Although the roadway mode is undesired in in-seam reflection seismic, it still carries useful information about the elastic properties of the excavation damaged zone (EDZ) – the fractured rock mass surrounding the roadway [38-40]. The extent and mechanical properties of the EDZ are crucial in roadway maintenance. However, there is still a lack of non-invasive and cost-effective methods to image and monitor EDZ. The roadway mode waveform changes due to EDZ were mentioned by Krajewski et al. [37].

In this paper, we analyze the propagation of seismic waves in the vicinity of a coal mine roadway as a cylindrically shaped excavation using 3-D seismic modelling. We extend previous numerical studies on the roadway mode [17, 35] by adding EDZ to the model. This allows for a more accurate simulation of the real-world underground conditions. We analyze particle motion in the center of the seam, similar to most of the in-seam seismic measurements. We use parallel viscoelastic finite-difference modelling code [41]. Properties of the roadway mode from modelling are further confirmed by the real data from the underground experiment. We observe a strong connection between the mechanical quality of the sidewall and changes in the roadway mode properties expressed in the group velocity – frequency domain. Implications of our results are twofold. They can be useful for the acquisition design of the in-seam seismic surveys. They also bring new insights into the roadway mode behavior, which are necessary to make a step towards imaging and monitoring the EDZ in an underground mine.

2. Methods

2.1. Finite-difference modelling

We use the viscoelastic finite-difference (FD) method [42] implemented in SOFI3D open-source modelling code to simulate the wave propagation in the vicinity of the roadway with the

presence of the EDZ. We set the distance between grid points in all models to 0.05 m as the optimum value [17]. We apply fourth-order spatial operator and second-order temporal operators on a staggered grid [43] and monitor the velocity of particle motion in each grid point within the receiver line with a time step equal to $1x10^{-6}$ s. We start from a simple model of an undisturbed low-velocity coal seam embedded between two homogeneous, isotropic half-spaces (Fig. 1).

The physical parameters of the model are listed in Tab. 1. The parameters are typical for Upper Silesia and this part of Europe, where the host rocks consist mainly of shale or sandstone and where the exploitation reaches more than 1 km nowadays [17, 27, 44]. Attenuation expressed as individual quality factors for P- and S-waves are set according to Krey et al. [45] and Anderson et al. [46]. We consider two scenarios that differ by the direction of the source excitation (modeled as horizontal force). It helps us to illuminate the different types of channel waves better. The first scenario (Fig. 1a) privileges Love-type channel wave excitation, while the second scenario (Fig. 1b) models Rayleigh-type channel wave.

Table 1

Simple rock-coal-rock model physical parameters.

	Thickness (m)	Vp (m/s)	Vs (m/s)	Density (kg/m^3)	Qp	Qs
Host rock (upper half-space)		4500	2600	2600	350	140
Coal seam	2	2400	1400	1400	150	60
Host rock (upper half-space)		4500	2600	2600	350	140
Roadway	5	0	0.0001	1250	10e10	10e10

In the next step, we add a 5-m diameter circular roadway centered in the middle of the model, i.e. in the coal seam (Fig. 2a). Finally, we set up the EDZ, which is a linear decrease of the

velocity and density down to 70% of their initial values for the undisturbed model (Fig. 2b). The width of the EDZ is 3 m [47, 48]. In both examples, the receivers are placed in the middle of the roadway and the coal seam, 10 cm from the sidewall, to simulate a typical in-seam seismic survey. A free surface around the roadway is created by setting vacuum parameters inside the roadway. It is not a perfect free surface condition, but it guarantees similar results and stable computation [42]. We use sinus wavelet (*s)* as a source, which is expressed as:

$$s = 0.75\pi f_c \sin(\pi t f_c)^3, \quad (1)$$

where t denotes time and f_c – central frequency. This wavelet has a broader frequency band than the Ricker wavelet, therefore producing much wider responses to track dispersive properties of seismic waves. The standard frequency range for exciting seismic waves for in-seam seismic measurement using blast or hammer is between 100-300 Hz. Therefore, we set the center frequency to 250 Hz, except the second scenario (Fig. 1b) where we set it to 370 Hz. The high frequency of the source in the second scenario helps to retrieve the Rayleigh-type channel wave with dispersion curves starting at much higher frequencies than the Love wave [49].

2.2. Dispersion curve computation for guided waves

To examine the dispersive waves around the roadway with the EDZ, we introduce the dispersion curves computation methods for channel waves. From the practical point of view, only the fundamental and the first higher modes of the channel waves are used to detect discontinuities as they can travel the greatest distances of all modes that are recorded in the coal seams [27]. Moreover, these two modes appear in the frequency range available for a blast or a hammer strike source. Therefore, we focus our analysis on these modes. Because of the similar elastic parameters for the floor and the roof of the seam in our models (Fig. 1 and 2), our analytical solution is obtained for similar homogenous half-spaces.

For a Love-type channel wave, we use the phase recursion algorithm [34]. Assuming that we have two similar homogenous half-spaces, the angular frequency ω is changing with respect to phase velocity c, for a coal thickness H as follows:

$$\omega(c) = \frac{2\arctan\left(i\frac{\rho_1 {V_{S1}}^2 \gamma_1}{\rho_2 {V_{S2}}^2 \gamma_2}\right) - n\pi}{H\gamma_2}, \tag{2}$$

where:

n - mode number (0 for fundamental order mode, 1 for first higher mode), i – imaginary unit,

ρ_1, ρ_2 – densities of rock and coal, respectively, V_{S1}, V_{S2} – S-wave velocities of rock and coal, respectively,

$\gamma_m = \sqrt{\frac{1}{Vs_m^2} - \frac{1}{c^2}}$ - propagation factor where $m = 1$ for host rock and $m = 2$ for coal. The equation can be solved when $V_{S1} > c > V_{S2}$.

The Rayleigh-type channel wave dispersion calculation was introduced in Buchanan [49] and Yang et al. [50]. In comparison to the Love-type channel wave (pure S-wave horizontally polarized), the solution for Rayleigh-type channel wave (P-wave plus S-wave vertically polarized = SV wave) is more complex and also includes P-wave velocity (V_P). Following Yang et al. [50], the Rayleigh-type channel wave dispersion equation can be solved by finding the determinants of the matrix M, i.e. $\det(M) = 0$, where

$$M = \begin{bmatrix} -iksh\left(\alpha_2\frac{H}{2}\right) & \beta_2 sh\left(\beta_2\frac{H}{2}\right) & -ik & \beta_1 & 0 & 0 & 0 & 0 \\ \alpha_2 ch\left(\alpha_2\frac{H}{2}\right) & ikch\left(\beta_2\frac{H}{2}\right) & -\alpha_1 & -ik & 0 & 0 & 0 & 0 \\ B_2 ch\left(\alpha_2\frac{H}{2}\right) & -A_2 sh\left(\beta_2\frac{H}{2}\right) & -B_1\frac{\rho_1}{\rho_2}\left(\frac{v_{S1}}{v_{S2}}\right)^2 & A_1\frac{\rho_1}{\rho_2}\left(\frac{v_{S1}}{v_{S2}}\right)^2 & 0 & 0 & 0 & 0 \\ -D_1 sh\left(\alpha_2\frac{H}{2}\right) & -C_2 sh\left(\beta_2\frac{H}{2}\right) & -\frac{\rho_1}{\rho_2}D_2 & -C_1\frac{\rho_1}{\rho_2}\left(\frac{v_{S1}}{v_{S2}}\right)^2 & 0 & 0 & 0 & 0 \\ 0 & 0 & 0 & 0 & 2ikch\left(\alpha_2\frac{H}{2}\right) & -2\beta_2 sh\left(\beta_2\frac{H}{2}\right) & -ik & -\beta_1 \\ 0 & 0 & 0 & 0 & 2\alpha_2 sh\left(\alpha_2\frac{H}{2}\right) & 2iksh\left(\beta_2\frac{H}{2}\right) & \alpha_1 & -ik \\ 0 & 0 & 0 & 0 & 2B_2 sh\left(\alpha_2\frac{H}{2}\right) & -2A_2 sh\left(\beta_2\frac{H}{2}\right) & B_1\frac{\rho_1}{\rho_2}\left(\frac{v_{S1}}{v_{S2}}\right)^2 & A_1\frac{\rho_1}{\rho_2}\left(\frac{v_{S1}}{v_{S2}}\right)^2 \\ 0 & 0 & 0 & 0 & 2D_1 ch\left(\alpha_2\frac{H}{2}\right) & 2C_2 ch\left(\beta_2\frac{H}{2}\right) & -\frac{\rho_1}{\rho_2}D_2 & C_1\frac{\rho_1}{\rho_2}\left(\frac{v_{S1}}{v_{S2}}\right)^2 \end{bmatrix}, \tag{3}$$

and

i - imaginary unit,

V_{S1}, V_{S2} – S-wave velocities of rock and coal, respectively,

$\alpha_m = \left[k^2 - \left(\frac{\omega}{V_{Pm}}\right)^2\right]^{1/2}$, $\beta_m = \left[k^2 - \left(\frac{\omega}{V_{Sm}}\right)^2\right]^{1/2}$ where $m = 1$ for host rock and $m = 2$ for coal

$A_1 = k^2 + {\beta_1}^2$, $A_2 = k^2 + {\beta_2}^2$,

$B_1 = 2ik\alpha_1$, $B_2 = 2ik\alpha_2$, $C_1 = 2ik\beta_1$, $C_2 = 2ik\beta_2$,

$D_1 = 2k^2 - \left(\frac{\omega}{V_{S2}}\right)^2$, $D_2 = 2\left(k\frac{V_{S1}}{V_{S2}}\right)^2 - \left(\frac{\omega}{V_{S2}}\right)^2$ where wavenumber $k = \frac{\omega}{c}$.

The group velocity dispersion curves can be obtained by differentiation of the phase velocity [27]. For the model parameters listed in Tab. 1, the dispersion curves for the two first modes are shown in Fig. 3. The characteristic Airy phase minimum is observed.

3. Numerical study

The numerical simulation results are presented in the frequency-wavenumber domain (F-K) computed for all traces along the receiver line (Fig. 1 and 2, blue line) by using a 2-D Fourier transform. To track changes within the Airy phase, we also analyze group velocity vs. frequency. Group velocity dispersion curves can be obtained using the multiple filtering techniques [51, 52]. We measure group velocity changes for seismic trace recorded 40 m away from the source, where dispersive waves are fully-formed and separated from body waves. We compute theoretical group and phase velocity dispersion curves for channel waves and body waves velocity limits to aid the interpretation (Fig. 3-6). In the case of the model with the roadway mode with- and without the EDZ, we also present polarization analysis for the horizontal plane (Fig. 5-6). The hodograms of particle motion are obtained from individually

filtered traces for short time-frequency windows with a step of 200 m/s and 100 Hz. Polarization helps us to find out what kind of waves the roadway mode consists of.

3.1. Undisturbed coal seam

Results simulating an undisturbed coal seam are presented in Fig. 4. We use these results as our reference for more complex simulations described later on. In general, one can note a coincidence between the theoretical dispersion curves and the main energy of the waves which are passing through the coal seam. In the case of the first scenario (Fig. 1a), where we analyze Y-component particle motion, the robust fundamental mode (M0) of Love-type channel wave can be observed with the minimum group wave velocity (Airy phase) of about 410 Hz (Fig. 4a and b). In the case of the second scenario (Fig. 1b) for the Z-component (Fig. 4c and d), we observe that the main energy travels as M0 of Rayleigh-type channel wave with the Airy phase about 610 Hz. A small portion of the energy is present in the first higher mode (M1) (Fig. 4d). On the contrary, for the X-component (Fig. 4e and f), maximum energy is gathered around M1 of the Rayleigh-type channel wave.

Both examples confirm that the Rayleigh-type channel wave amplitudes reach maximum values for M0 for Z-component and M1 for the X-component in the middle of the coal seam [27]. It is worth noting that even though the properties of the coal seam included moderate attenuation (Qp = 150, Qs = 60), the dominant energy in the wavefield recorded 40 m from the source is still belonging to the normal modes (i.e. modes which propagate inside the coal) rather than the leaky modes (modes connected with the energy released outside the coal seam).

3.2. Coal seam and a roadway

When we simulate a roadway in the middle of the coal seam (Fig. 2a), we observe the dispersive wave on the horizontal components (Fig. 5) quite similar to the M0 of Love-type

channel wave for undisturbed coal seam (compare with Fig. 4a and b). It only differs from the phase and group velocity, which are about 10% lower. Such a dispersive mode is called the roadway mode [35,37]. The interesting feature of the roadway mode is that the leading energy is still gathered around the Airy phase of the Love-type channel wave with the group velocity comparable with the Airy phase of Rayleigh-type channel wave M0 (Fig. 5b). The hodograms (see the thin red line in Fig. 5d) show the elliptical nature of particle motions for the roadway mode in the horizontal plane in the center of the seam. Indeed, horizontal components recorded close to the sidewall in the center of the seam, besides from Love-type channel wave, should also contain elliptically-polarized Rayleigh-type surface tunnel waves (for X- and Y-component) and a higher mode of Rayleigh-type channel wave (X-component). However, the second one does not appear due to the direction of the source (normal to the sidewall like hammer strike) and its central frequency. The ellipses around the main energy (Airy phase) are stretched towards the Y-direction up to about twice the amplitude of the X displacement. The higher amplitudes of roadway mode can be visible also on the seismic records on the Y component (Fig. 5b). It confirms that the Love-type channel wave is contaminated with the Rayleigh surface tunnel wave**.**

3.3. Coal seam, roadway and the EDZ

In Fig. 6, we present our numerical simulation results for the model that includes the roadway and the EDZ (Fig. 2b). The reduction of elastic parameters within the EDZ produces a slower coal seam wave train, hence the velocity decrease of the roadway mode is visible in both the F-K and group velocity-frequency plots. It can be seen that the main energy is still gathered around the Love-type channel wave (Airy phase) of M0 (Fig. 6b). In Fig. 6, we add two other theoretical dispersion curves for M0 of Rayleigh (solid blue line) and Love (solid red line) surface waves computed for the 1-D model of the coal seam with the EDZ, excluding host rock layers. To

compute these dispersion curves we used Geopsy software [53]. In the F-K domain, we notice that for the higher frequencies, the wave is traveling as an M0 of the Rayleigh surface tunnel wave. It is due to the smaller wavelength of waves, which cannot be affected by the host rocks and propagate only inside the coal seam. However, for lower frequencies, where the channel waves dominate the wavefield, we observe significant velocity reduction, especially visible for the group velocity domain (Fig. 6b). Group velocity is becoming even lower than the lowest group velocity on the theoretical dispersion curves for surface waves for a coal seam in the absence of host rocks but with the EDZ. It confirms that the Love-type channel wave strongly influences the roadway mode propagation velocity in the horizontal plane. Polarization for the selected trace for the horizontal plane is similar to the one observed for the roadway mode without the EDZ. One can also observe that the roadway mode with the presence of the EDZ is less dispersive, i.e. it travels with a velocity of ~750 m/s over a broad spectrum (from 300 to 500 Hz). Despite the moderate intrinsic attenuation in the model, the roadway mode is still strong and dominates in the horizontal components at a 40 m distance from the source, making it very promising in terms of imaging of the EDZ in a coal mine.

4. Real-data application

4.1. Mining and seismic survey settings

In order to see if the roadway mode properties from numerical modelling are confirmed by the real data, we arranged an underground experiment. It was carried out in the Rydułtowy coal mine in Poland. One seismic profile was set in the roadway III-1200-E1 in the 713/1-2 coal seam (Fig. 7a). The coal layer is about 2.8 m thick in this place. The coal seam dips at about 9 degrees towards the west. The floor and the roof are mainly composed of claystone and sandstone. Above the roadway E1, few mine-out areas exist (Fig. 7a, gray areas limited by the dashed line). The nearest one (703/1-2) is about 100 m above, and the other two (620, 624) are more than 400 m away. The roadway E1 was extracted at the beginning of 2020. Due to the

stress concentration within the existing remnants located close to the roadway 4b-E1, the torpedo blasting was done in three boreholes. Torpedo blasting (long-hole destress blasting) is a routine approach to reduce stress concentrations occurring in the rock mass. As a consequence, the sidewall in this area is fractured. Our seismic profile is set in both damaged (below the remnants) and undamaged (below the gobs) zones to catch differences in the roadway mode propagation parameters.

We used 12 horizontal-component geophones with a natural frequency of 14 Hz (Fig. 7a, blue triangles). The distance between geophones was 3 m. The sampling frequency was set to 4kHz. Each geophone was mounted normal to the sidewall (the same as Y-component in modelling case) on the 40 cm rod to guarantee a good coupling with the coal seam. We generated seismic waves using 25 shot points along the profile with a sledgehammer (Fig 7a, red arrows). The disctace between shot points was 3 m. In Fig. 7b, the example of seismic record measured for source S05 is shown. The strong dispersive wave is visible, which resembles roadway modes from Fig 5a and 5b. For the hammer source used in this study, the dominant energy of roadway mode speaks around 200 Hz.

4.2. Data overview

In Fig. 8a, we present 23 seismic traces for the same 21 m shot-receiver distance (i.e. common-offset gather). The raw data are shown without any changes within amplitude and frequency ranges. One can see that the traces at the beginning of the seismic profile differ significantly from those at the end. The arrival times of seismic waves are much earlier for the first 30 m compared to those at the end of the profile. Also, time differences between consecutive peaks and troughs of waveforms are much shorter at the first tens of meters, suggesting the predominance of higher frequencies. In Fig. 8b, we show the example of a roadway mode by transforming the red trace marked in Fig. 8a to group velocity – frequency

domain. The dispersive nature of a roadway mode is observed (see red points in Fig. 8b). The maximum energy is located at about 270 Hz, where group velocity is relatively low (see red circle in Fig. 8b). A similar feature of a roadway mode was observed in modelling (compare e.g. with Fig. 5 & 6).

4.3. Results

Our survey layout with the dense shots provides a unique opportunity to track changes in the roadway mode with an offset along the profile. In Fig. 9a and 9b, we present how group velocity and frequency of maximum energy of a roadway mode change, respectively. In general, for offsets smaller than 10 m, we observe lower group velocity for the whole profile (Phase 1). It is mainly because the roadway mode does not excite in the entire frequency spectrum at such a short distance and is still mixed with body waves (near-field effect) [54]. At the same time, the wavelength in Phase 1 is up to 2 m (Fig. 9c), therefore seismic waves penetrate the most external part of the EDZ (the most fractured). In Phase 1 (i.e. for small offsets), the group velocity does not depend on frequency, confirming that body waves dominate in the wavefield. From intermediate offset between 10 m and about 32 m (Phase 2), where roadway mode is fully formed and propagates as a strong bundle of dispersive waves (as shown in modelling example in Fig. 5 and 6), the group velocity changes and corresponds to the mechanical quality of rock mass. Conseqeuntly, in the undamaged zone, the roadway mode group velocity is about 500 m/s and in the fractured zone it is about 300 m/s. These changes are also observed in the raw waveforms (Fig. 8a). In Phase 2, the wavelength is mainly between 1.5 and 3.5 m. The group velocity of Phase 2 depends on the frequency (which is typical behavior for dispersive waves). For the largest offsets greater than 32 m (Phase 3), we observe a gradual increase of the roadway mode frequency along the profile, similar to those in Phases 1 and 2. However, the group velocity is much higher than in Phases 1 and 2. It is mainly due to

the roadway mode attenuation and the modes excited in the surrounding rocks. After 32 m, the wave energy leaks to the surrounding rocks, hence the wavelength is much longer, and group velocity increases. Based on these observations, we can conclude that in our case, the most optimal offsets for imaging the EDZ with the use of the roadway mode are those in Phase 2, i.e. from 10 m to 32 m.

In Fig. 10a, we present dispersive curves of roadway mode for traces with an offset equal to 21 m (for all traces shown in Fig. 8a). We pick them similarly to the example in Fig. 8b (red points). The curves for traces recorded by the same geophone for sources with the same offsets but different (opposite) shot locations are averaged. The mid-point between shot and receiver is set as a location of the curve along the seismic profile. We notice similar changes to those in Fig. 9. For the first 38 m of the profile, the roadway mode characterizes higher group velocities. The highest values are observed at the beginning of the profile, where the sidewall is undamaged and stable. The lowest group velocities are noticed after 40 m of the profile, below the remnants, and close to the part of rock mass that was fractured by torpedo blasting. In Fig. 10b, we show the average group velocity and the standard deviation for each dispersion curve shown in Fig. 10a. The average group velocity changes between the undamaged and damaged part of the sidewall are robust and reach up to 550 m/s. The standard deviations computed for each dispersion curve for the frequency range of 100-700 Hz are relatively low (from about 20 m/s to about 90 m/s) . This observation is in agreement with numerical results (Fig. 6) that show relatively low dispersivity withing EDZ.

5. Discussion and conclusions

We examined the behavior of seismic waves that propagate inside the coal seam in the vicinity of the roadway sidewall affected by the EDZ. To this end we used numerical

simulations and real data from the underground experiment. We focused on the most substantial dispersive waves and their so-called roadway mode.

Our 3-D FD modelling emphasizes the prominent features of a roadway mode in a coal seam and shows the new ones that can help to image of the EDZ and to plan an in-seam seismic survey. We can summarize our modelling observations as follows: (i) when the source (strike) is located just close to the sidewall (typical for in-seam seismic surveys), the roadway mode in the center of the seam dominates on the horizontal components, particularly on the component normal to the sidewall; (ii) roadway mode in a horizontal plane in the center of the seam consitis of the mixed Rayleigh surface tunnel wave and Love-type channel wave; (iii) the main energy of a roadway mode is focused around the Airy phase of the fundamental mode Love-type channel wave. However, when there is no EDZ, the velocity of roadway mode is 10% lower, and the minimum group velocity is comparable with the Airy phase of the fundament mode of Rayleigh-type channel wave. When the EDZ is present, the minimum group velocity strongly decreases, and it is even lower than the minimum group velocity of Rayleigh and Love surface waves in a coal seam; (iv) even though the absorption is included in the model, the roadway mode still remains prominent at largest offsets. This feature should be considered when planning in-seam seismic reflection measurements, mainly when the expected discontinuities are located close to the sidewalls. When someone wants to use channel waves to look ahead new extracted roadway, it is better to put the source and receiver deeper into the undisturbed coalbed. In other cases, velocity reduction of the channel wave due to the roadway mode should be accounted for during data processing and imaging, e.g. in migration procedure; (v) the roadway mode within EDZ is less dispersive than without EDZ i.e. has a similar group velocity in the broader frequency band. This feature can be used to image and monitor the rock mass deformation close to the sidewall.

With the real-data application, we confirmed the roadway mode features observed in the synthetic data, and we demonstrated how this mode reacts to the rock mass deformation within the EDZ. The significant group velocity changes within EDZ highlighted the strong dependence of this dispersive wave from the mechanical state of the EDZ. However, it is important to note that if one wants to use it to image or monitor the sidewall mechanical quality, one should first choose the right offset range to avoid near-field effects or energy leakage to the surrounding rocks. In our underground experiment, the optimal offset was 21 m. Roadway mode is easy to identify due to its high signal-to-noise ratio, hence it is less prone to errors during processing and interpretation. Moreover, roadway mode in a horizontal plane consists mainly of a shear wave, which is more sensitive to any structural changes in the rock mass than the P-wave, therefore it is especially suitable for monitoring. We showed that using single horizontal geophone with the fixed source-receiver distance is sufficient to determine the group velocity dispersion curves of the roadway mode. Thus, our methodology is very practical tool for in-mine measurements. Acquisition with such fixed-offset geometry with a hammer as a source is fast, inexpensive, and involves a small crew. Such measurements can be applied in a time-lapse mode to track relative group velocity changes inside the EDZ to maintain the underground excavations while mining and improve safety in underground mines. Since the main requirement for roadway mode measurements is the presence of horizontal stratigraphy and low-velocity waveguide, our methodology is not limited to the coal mines and may be useful broader mineral exploration context.

Acknowledgments

This research is supported by the Polish National Science Centre grant no UMO-2018/30/Q/ST10/00680. We thank two anonymous reviewers for their constructive comments.

References

[1] Ben-Zion Y. Properties of seismic fault zone waves and their utility for imaging low-velocity structures. J. Geophys. Res. Solid Earth 1998;103:12567-12585. https://doi.org/10.1029/98jb00768.

[2] Jahnke G, Igel H, Ben-Zion Y. Three-dimensional calculations of fault-zone-guided waves in various irregular structures. *Geophys. J. Int.* 2002;151:416-426. https://doi.org/10.1046/j.1365-246X.2002.01784.x.

[3] Furumura T, Kennett BLN. Subduction zone guided waves and the heterogeneity structure of the subducted plate: Intensity anomalies in northern Japan. *J. Geophys. Res. Solid Earth* 2005;110:1-27. https://doi.org/10.1029/2004JB003486.

[4] Evison FF. A coal seam as a guide for seismic energy. *Nature* 1955;176(4495):1224-1225. https://doi.org/10.1038/1761224a0.

[5] Krey T. Channel waves as a tool of applied geophysics in coal mining. *Geophysics* 1963;28:701-714. https://doi.org/10.1190/1.1439258.

[6] Buchanan DJ. The propagation of attenuated SH channel waves. *Geophys. Prospect*. 1978;26:16-28. https://doi.org/10.1111/j.1365-2478.1978.tb01575.x.

[7] Li X, Schott W, Rutert H. Frequency-dependent Q-estimation of Love-type channel waves and the application of Q-correction to seismograms. *Geophysics* 1995;60:1773-1789. https://doi.org/10.1190/1.1443911.

[8] Buchanan DJ, Jackson PJ, Davis R. Attenuation and anisotropy of channel waves in coal seams. *Geophysics* 1983;48:133-147. https://doi.org/10.1190/1.1441453.

[9] Ji G, Li H, Wei J, Yang S. Preliminary study on wave field and dispersion characteristics of channel waves in VTI coal seam media. *Acta Geophys.* 2019;67:1379-1390. https://doi.org/10.1007/s11600-019-00326-x.

[10] Liu E, Crampin S, Roth B. Modelling channel waves with synthetic seismograms in an anisotropic in-seam seismic survey. *Geophys. Prospect*. 1992;40:513-540. https://doi.org/10.1111/j.1365-2478.1992.tb00539.x.

[11] Asten MW, Drake LA, Edwards S. In-seam seismic Love wave scattering modeled by the finite element method. *Geophys. Prospect.* 1984;32:649-661. https://doi.org/10.1111/j.1365-2478.1984.tb01711.x.

[12] Breitzke M, Dresen L. Love-type seam-waves in washout models of coal seams. *Geophys. Prospect.* 1986;34:1167-1184. https://doi.org/10.1111/j.1365-2478.1986.tb00521.x.

[13] Edwards SA, Asten MW, Drake LA. P-SV wave scattering by coal-seam inhomogeneities. *Geophysics* 1985;50:214-223. https://doi.org/10.1190/1.1441911.

[14] He W, Ji G, Dong S, Li G. Theoretical basis and application of vertical Z-component in-seam wave exploration. *J. Appl. Geophys.* 2017;138:91-101. https://doi.org/10.1016/j.jappgeo.2017.01.008.

[15] Kerner C, Dresen L. The influence of dirt bands and faults on the propagation of Love seam waves. *J. Geophys. - Zeitschrift fur Geophys*. 1985;57:77-89. https://doi.org/10.23689/fidgeo-3511.

[16] Korn M, Stockl H. Reflection and transmission of Love channel waves at coal seam discontinuities computed with a finite difference method. *J. Geophys. - Zeitschrift fur Geophys*. 1982;50:171-176. https://doi.org/10.23689/fidgeo-3505.

[17] Essen K, Bohlen T, Friederich W, Meier T. Modelling of Rayleigh-type seam waves in disturbed coal seams and around a coal mine roadway. *Geophys. J. Int*. 2007;170:511-526. https://doi.org/10.1111/j.1365-246X.2007.03436.x.

[18] Li H, Zhu P, Ji G, Zhang Q. Modified image algorithm to simulate seismic channel waves in 3D tunnel model with rugged free surfaces. *Geophys. Prospect*. 2016;64:1259-1274. https://doi.org/10.1111/1365-2478.12351.

[19] Yang ST, Wei JC, Cheng JL, Shi LQ, Wen ZJ. Numerical simulations of full-wave fields and analysis of channel wave characteristics in 3-D coal mine roadway models. *Appl. Geophys.* 2016;13:621-630. https://doi.org/10.1007/s11770-016-0582-9.

[20] Dresen L, Kerner C, Kuhbach B. The influence of an asymmetry in the sequence rock / coal / rock on the propagation of Rayleigh seam waves. *Geophys. Prospect*. 1985;33:519-539. https://doi.org/10.1111/j.1365-2478.1985.tb00765.x.

[21] Freystatter S, Dresen L. The influence of oblique dipping discontinuities on the use of Rayleigh channel waves for the in-seam seismic reflection method. *Geophys. Prospect.* 1978;26:1-15. https://doi.org/10.1111/j.1365-2478.1985.tb00765.x.

[22] Gritto R, Dresen L. Seismic modelling of seam waves excited by energy transmission into a seam. *Geophys. Prospect.* 1992;40:671-699. https://doi.org/10.1111/j.1365-2478.1992.tb00547.x.

[23] Mason IM, Buchanan DJ, Booer AK. Channel wave mapping of coal seams in the United Kingdom. *Geophysics* 1980;45(6):1131-1143. https://doi.org/10.1190/1.1441112.

[24] Schott W, Waclawik P. On the quantitative determination of coal seam thickness by means of In-Seam Seismic Surveys. *Can. Geotech. J.* 2015;52:1496-1504. doi/abs/10.1139/cgj-2014-0466.

[25] Zhu M, Cheng J, Cui W, Yue H. Comprehensive prediction of coal seam thickness by using in - seam seismic surveys and Bayesian kriging. *Acta Geophys.* 2019;67:825-836. https://doi.org/10.1007/s11600-019-00298-y.

[26] Buchanan DJ, Davis R, Jackson PJ, Taylor PM. Fault location by channel wave seismology in United Kingdom coal seams. *Geophysics* 1981;46:994-1002. https://doi.org/10.1190/1.1441248.

[27] Dresen L, Ruter H. Seismic coal exploration. Part B: in-seam seismics. 1994; https://doi.org/10.1016/0148-9062(96)87542-5.

[28] Lüth S, Buske S, Giese R, Goertz A. Fresnel volume migration of multicomponent data. *Geophysics* 2005;70:S121-S129. https://doi.org/10.1190/1.2127114.

[29] Lüth S, Giese R, Otto P, Krüger K, Mielitz S, Bohlen T, Dickmann T. Seismic investigations of the Piora Basin using S-wave conversions at the tunnel face of the Piora adit (Gotthard Base Tunnel). Int. *J. Rock Mech. Min. Sci.* 2008;45:86-93. https://doi.org/10.1016/j.ijrmms.2007.03.003.

[30] Hu Y, McMechan GA. Imaging mining hazards within coalbeds using prestack wave equation migration of in-seam seismic survey data: A feasibility study with synthetic data. *J. Appl. Geophys.* 2007;63:24-34. https://doi.org/10.1016/j.jappgeo.2007.03.002.

[31] Ji G, Wei J, Yang S, Li X, Bai J, Sui Y. Three-component polarization migration of channel waves for prediction ahead of coal roadway. *J. Appl. Geophys.* 2018;159:475-483. https://doi.org/10.1016/j.jappgeo.2018.09.028.

[32] Wang B, Liu S, Zhou F, Lu T, Huang L, Gao Y. Polarization migration of three-component reflected waves under small migration aperture condition. *Acta Geodyn. Geomater.* 2016;13:47-58. https://doi.org/10.13168/AGG.2015.0049.

[33] Wang B, Sun H, Huang L, Liu S, Jin B, Zhang H, Ding X, Qiu W, Wang S. Wave Field Characteristics of Small Faults around the Loose Circle of Rock Surrounding a Coal Roadway. *J. Environ. Eng. Geophys.* 2020; 25:245-254. https://doi.org/10.2113/JEEG19-073.

[34] Rader D, Schott W, Ruter H. Calculation of dispersion curves and amplitude-depth distributions of love channel waves in horizontal-layered media. *Geophys. Prospect.* 1985;33:800-816. https://doi.org/10.1111/j.1365-2478.1985.tb00779.x.

[35] Lagasse PE, Mason IM. Guided modes in coal seams and their application to underground seismic surveying, in: Ultrasonics Symposium Proceedings IEEE Cat. 75 CHO 994-4SU, 1975:64–67.

[36] Jetschny S, Bohlen T, De Nil D. On the propagation characteristics of tunnel surface-waves for seismic prediction. *Geophys. Prospect.* 2010;58:245-256. https://doi.org/10.1111/j.1365-2478.2009.00823.x.

[37] Krajewski P, Dresen L, Schott W, Ruter H. Studies of roadway modes in a coal seam by dispersion and polarization analysis: a case history. *Geophys. Prospect.* 1987;35:767-786. https://doi.org/10.1111/j.1365-2478.1987.tb02257.x.

[38] Tsang CF, Bernier F, Davies C. Geohydromechanical processes in the Excavation Damaged Zone in crystalline rock, rock salt, and indurated and plastic clays - In the context of radioactive waste disposal. *Int. J. Rock Mech. Min. Sci.* 2005;42:109-125. https://doi.org/10.1016/j.ijrmms.2004.08.003.

[39] Schuster K, Amann F, Yong S, Bossart P, Connolly P. High-resolution mini-seismic methods applied in the Mont Terri rock laboratory (Switzerland). *Swiss J. Geosci.* 2017;110:213-231. https://doi.org/10.1007/s00015-016-0241-4.

[40] Zhu WC, Bruhns OT. Simulating excavation damaged zone around a circular opening under hydromechanical conditions. *Int. J. Rock Mech. Min. Sci.* 2008; https://doi.org/10.1016/j.ijrmms.2007.09.007.

[41] Bohlen T. Parallel 3-D viscoelastic finite difference seismic modelling. *Comput. Geosci.* 2002;28 887-899. https://doi.org/10.1016/S0098-3004(02)00006-7.

[42] Bohlen T, Saenger EH. Accuracy of heterogeneous staggered-grid finite-difference modeling of Rayleigh waves. *Geophysics* 2006;71:T109-T115. https://doi.org/10.1190/1.2213051.

[43] Virieux J. P-SV wave propagation in heterogeneous media: velocity-stress finite-difference method, *Geophysics*, 1986;51(4):889-901. https://doi.org/10.1190/1.1442147.

[44] Kokowski J, Szreder Z, Pilecka E. Reference P-wave velocity in coal seams at great depths in Jastrzebie coal mine. *E3S Web of Conferences* 2019;133 01011. https://doi.org/10.1051/e3sconf /201913301011.

[45] Krey T, Arnetzl H, Knecht M. Theoretical and practical aspects of absorption in the application of in-seam seismic coal exploration. *Geophysics* 1982;47:1645-1656. https://doi.org/10.1190/1.1441314.

[46] Anderson DL, Ben-Menahem A, Archambeau CB. Attenuation of seismic energy in the upper mantle. *J. Geophys. Res.* 1965;70:1441-1448. https://doi.org/10.1029/jz070i006p01441.

[47] Tian M, Han L, Meng Q, Jin Y, Meng L. In situ investigation of the excavation-loose zone in surrounding rocks from mining complex coal seams. *J. Appl. Geophys.* 2019;168:90-100. https://doi.org/10.1016/j.jappgeo.2019.06.008.

[48] Wang H, Jiang Y, Xue S, Shen B, Wang C, Lv J, Yang T. Assessment of excavation damaged zone around roadways under dynamic pressure induced by an active mining process. *Int. J. Rock Mech. Min. Sci.* 2015;https://doi.org/10.1016/j.ijrmms.2015.03.032.

[49] Buchanan DJ. Dispersion calculations for SH and P-SV waves in multilayered coal seams. *Geophys. Prospect.* 1987;35:62-70. https://doi.org/10.1111/j.1365-2478.1987.tb00802.x.

[50] Yang XH, Cao SY, Li DC, Yu PF, Zhang HR. Analysis of quality factors for Rayleigh channel waves. *Appl. Geophys.* 2014;11:107-114. https://doi.org/10.1007/s11770-014-0409-5.

[51] Dziewonski A, Bloch S, Landisman M. A technique for the analysis of transient seismic signals. *Bull. Seismol. Soc. Am.* 1969;59(1):427-444.

[52] Feng L, Zhang Y. Dispersion calculation method based on S-transform and coordinate rotation for Love channel waves with two components. *Acta Geophys.* 2017;65:757-764. https://doi.org/10.1007/s11600-017-0069-y.

[53] Wathelet M. An improved neighborhood algorithm: Parameter conditions and dynamic scaling. *Geophys. Res. Lett.* 2008;35:1-5. https://doi.org/10.1029/2008GL033256.

[54] Foti S, Lai CG, Rix GJ, Strobbia C. Surface wave methods for near-surface site characterization. 2014; CRC Press.

Figures

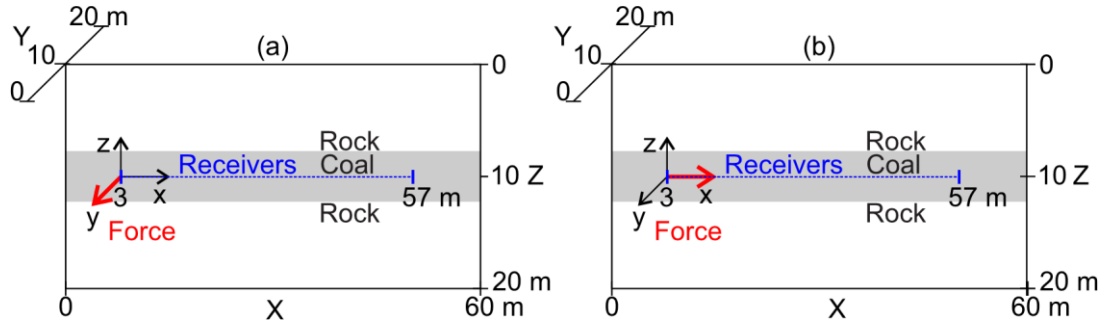

Fig. 1. Two modelling scenarios for the simple rock-coal-rock model: (a) horizontal-force source perpendicular to the receiver array and parallel to the roof/floor of a coal seam, (b) horizontal-force source parallel to the receiver array parallel to the roof/floor of a coal seam.

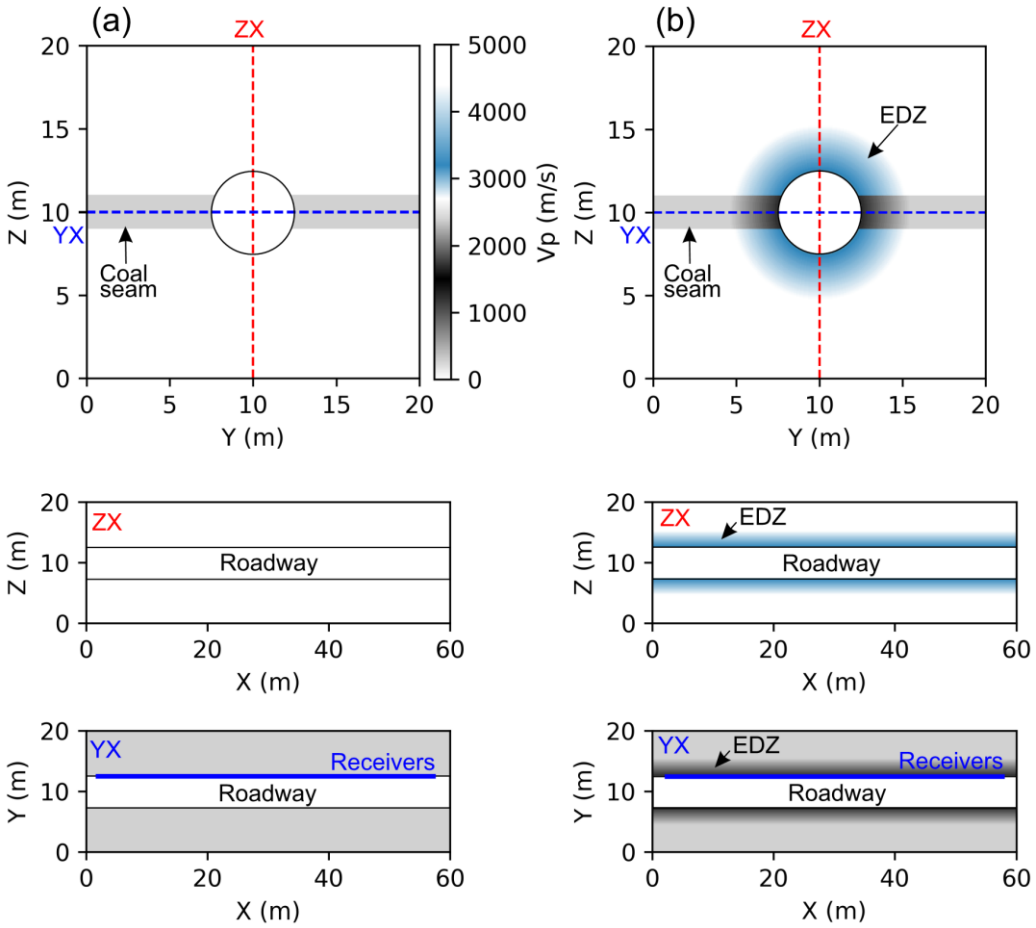

Fig. 2. An example of the P-wave velocity model of a roadway without (a) and with (b) EDZ.

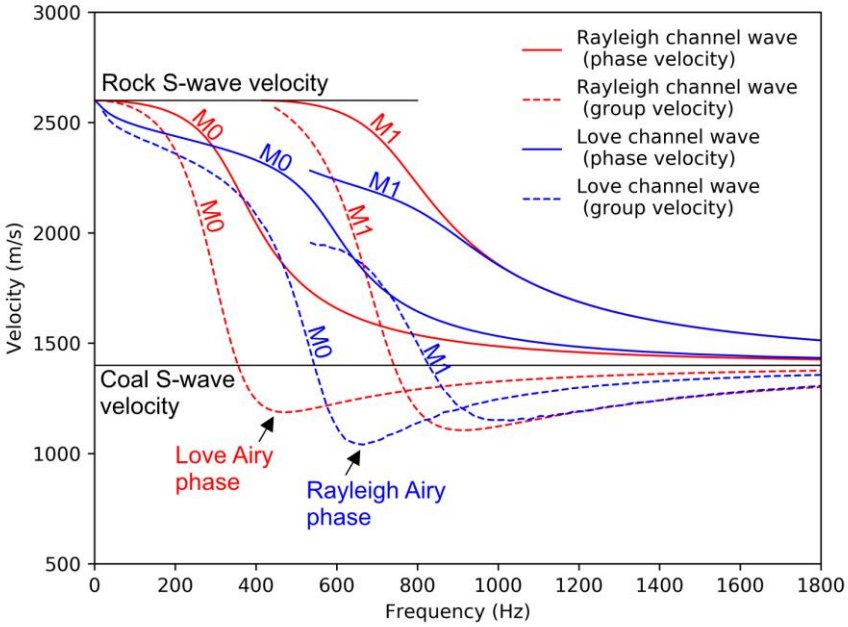

Fig. 3. Analytical phase and group velocity vs. frequency plot for the fundamental mode (M0) and first-higher mode (M1) of Love- and Rayleigh-type channel waves for model parameters in Tab. 1.

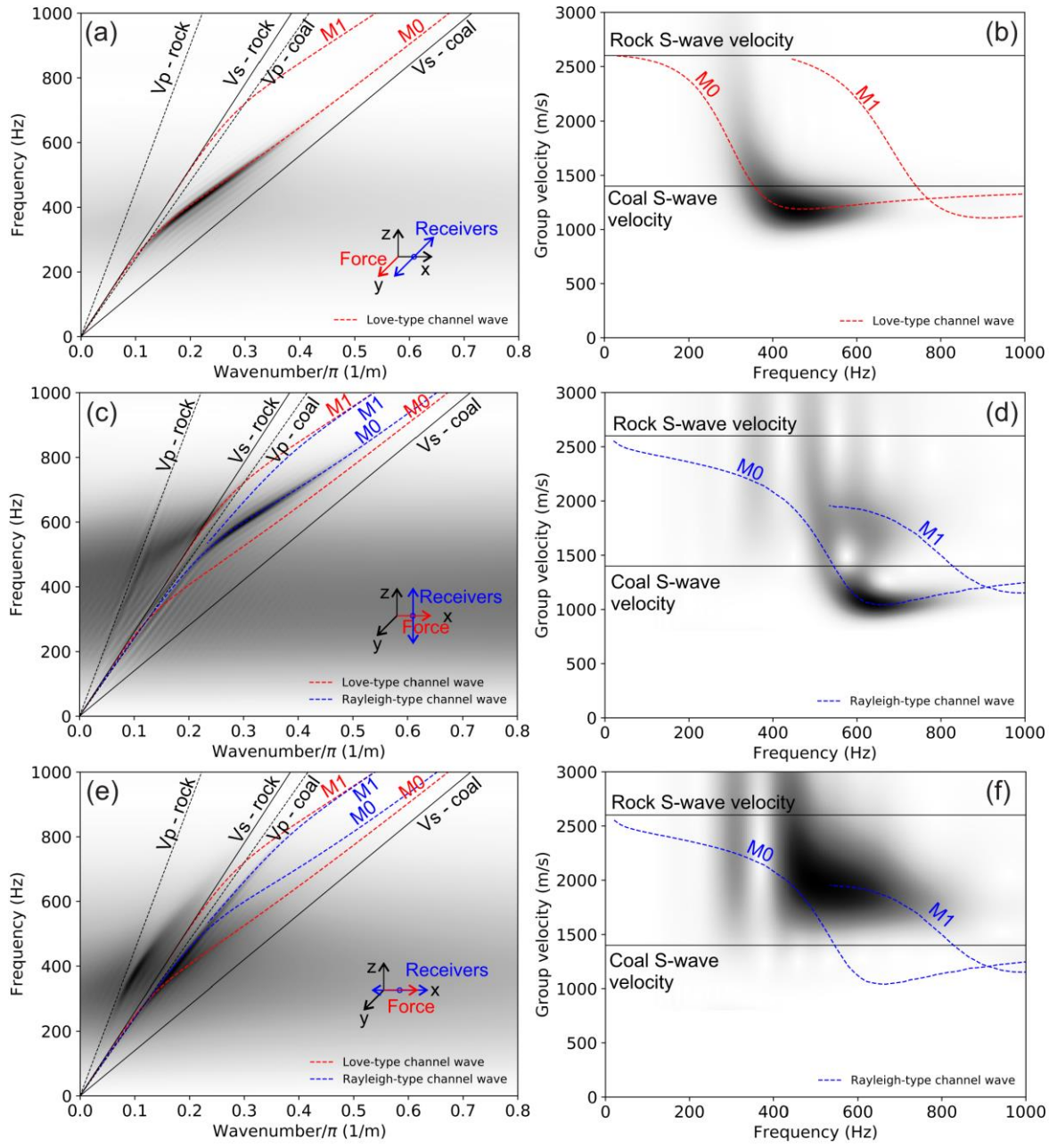

Fig. 4. Modelling results for an undisturbed coal seam in frequency-wavenumber (F-K) and group velocity – frequency domains. M0 and M1 denote fundamental mode and first higher mode, respectively. Blue and red dashed lines indicate Love- and Rayleigh-type channel waves, respectively. (a, b) – Y component of particle motion for the first scenario (Love-type channel wave); (c, d) – Z component of particle motion for the second scenario (M0 of Rayleigh-type channel wave); (e, f) – X component of particle motion for the second scenario (M1 of Rayleigh-type channel wave).

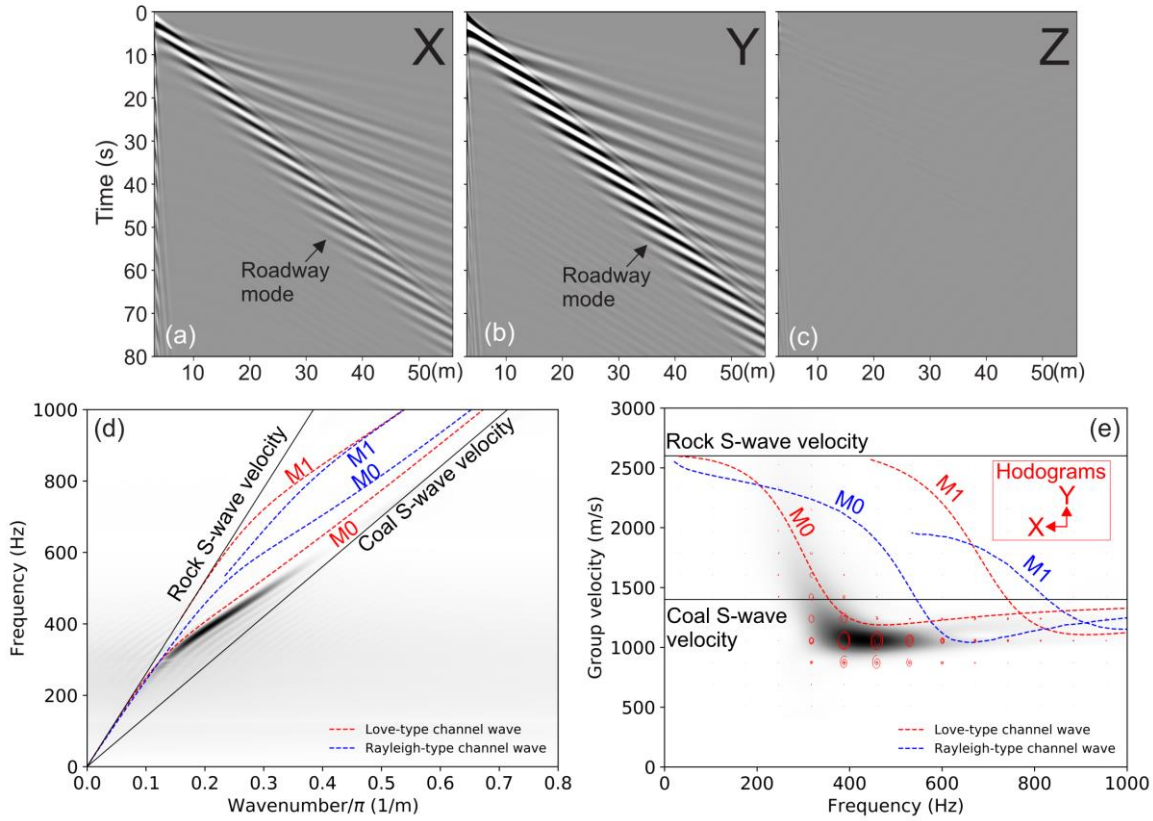

Fig. 5. Seismic records of X- (a), Y- (b), and Z-component (c) normalized to the maximum amplitude of Y for the model including cylindrically shaped roadway. A strong roadway mode is visible. Y-component in frequency-wavenumber (F-K) (d) and selected trace of Y-component 40 m away from the source group velocity – frequency domains (e). Blue and red dashed line indicate Love- and Rayleigh-type channel waves, respectively. The thin red line in (d) is the particle motion (hodograms) in a 2-D plane (X and Y).

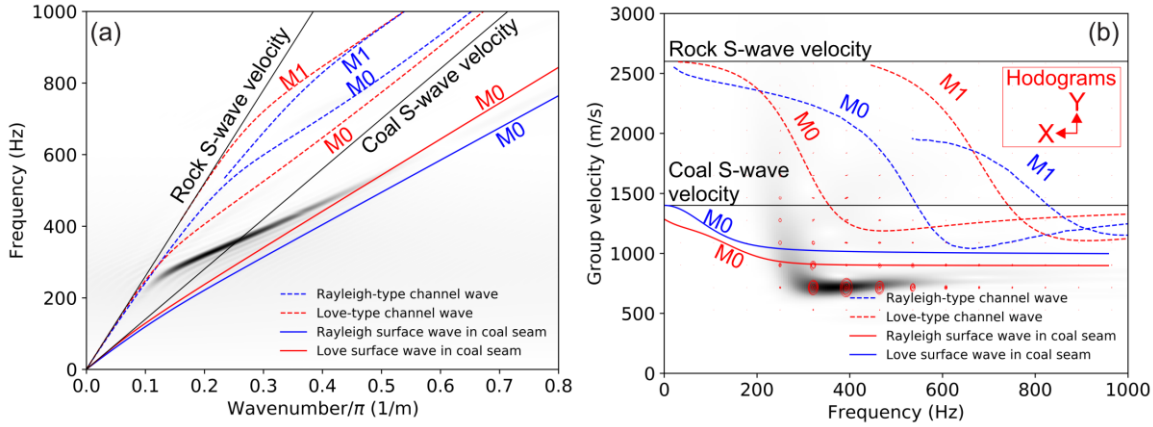

Fig. 6. Modelling results for the model including cylindrically shaped roadway and the EDZ in frequency-wavenumber (F-K) (a) and group velocity-frequency domains (b). Blue and red dashed lines indicate theoretical dispersion curves of Rayleigh- and Love-type channel waves, respectively. Blue and red solid lines are the theoretical dispersion curve of Rayleigh and Love surface waves. The thin red line in (b) is the particle motion (hodogram) in a 2-D plane (X and Y).

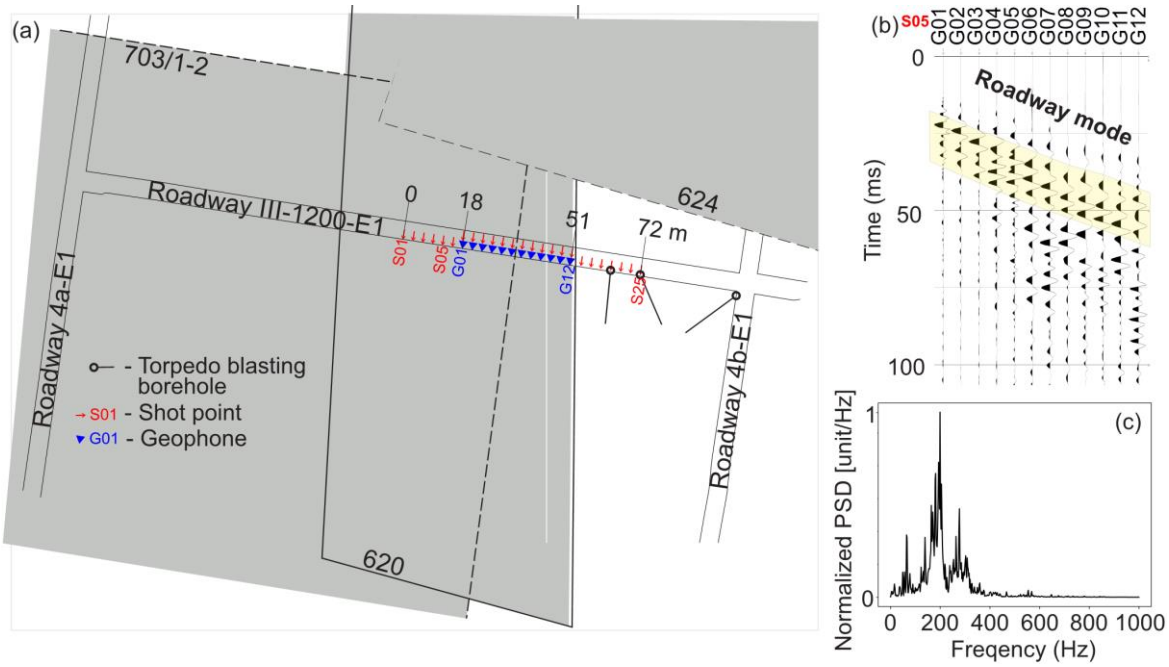

Fig. 7. Seismic survey layout and mining setting (a) together with (b) the example of the seismic record of the Y-component (normal to the sidewall) from source point S05.

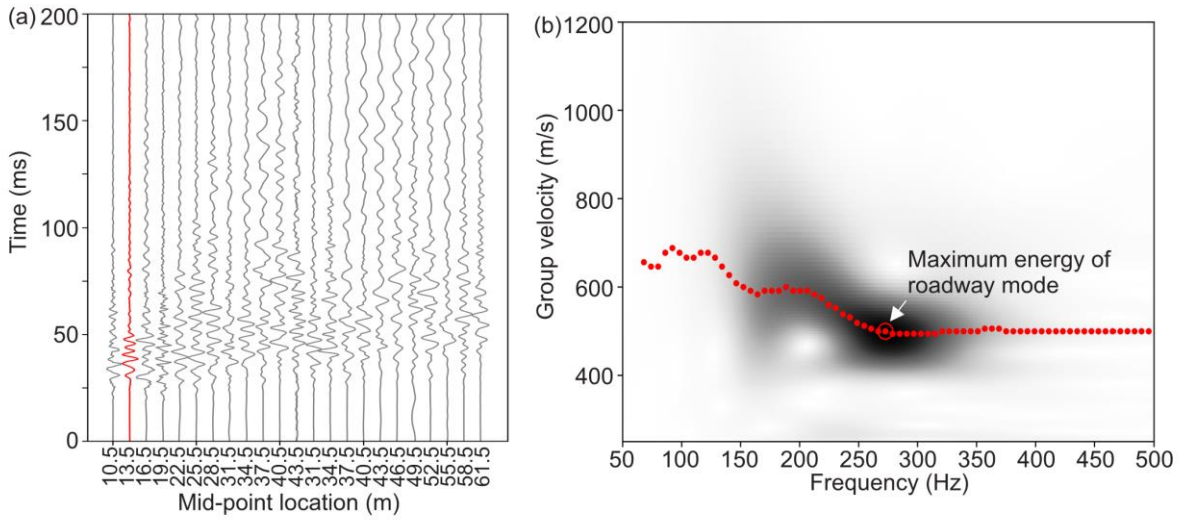

Fig. 8. (a) Common-offset seismic gather with different mid-points (points in a halfway from shot to receiver) along the seismic profile and (b) group velocity – frequency representation of the red trace marked in (a). Roadway mode dispersive points are marked by red dots with maximum energy around 270 Hz (red circle).

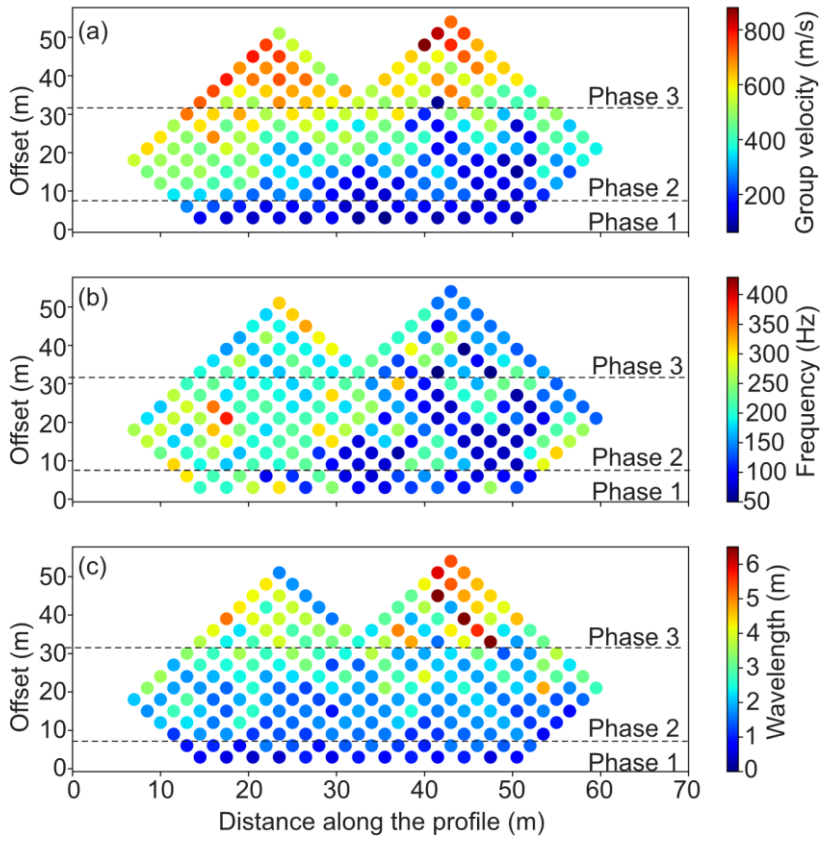

Fig. 9. (a) Group velocity, (b) frequency, and (b) wavelength of maximum energy of the roadway mode along with the seismic profile for different offsets.

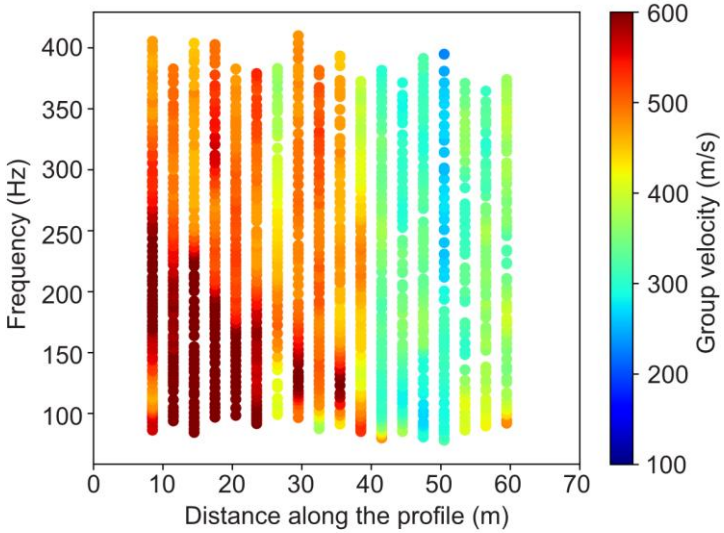

Fig. 10. Dispersion curves of a roadway mode along with the seismic profile for 21 m offset.